Biochimica et Biophysica Acta 857 (1986) 238–250
Elsevier

BBA 73100

Spectrofluorimetric study of porphyrin incorporation into membrane models – evidence for pH effects

Daniel Brault [a], Christine Vever-Bizet [b] and Trung Le Doan [a]

[a] *Laboratoire de Biophysique, INSERM U.201, CNRS UA.481, Muséum National d'Histoire Naturelle, 75005 Paris, and* [b] *Laboratoire de Physique, CNRS UA.491, Faculté de Pharmacie, Université Louis Pasteur, 67400 Illkirch-Graffenstaden (France)*

(Received December 2nd, 1985)

Key words: Porphyrin-membrane interaction; Membrane model; pH effect; Fluorescence

The effects of hydrophobicity and charges of dicarboxylic porphyrins upon their interactions with membrane model systems are investigated. Four protonation steps are evidenced from fluorescence emission studies of hematoporphyrin IX and its more hydrophobic parent compound lacking of alcoholic chain, deuteroporphyrin IX. They are attributed to the successive protonations of the inner nitrogens of the porphyrin cycle ($pK = 4.7$ and 2.9 for hematoporphyrin and 4.4 and 2.7 for deuteroporphyrin) and successive deprotonations of propionic groups ($pK \approx 5.0$ and 5.5 for hematoporphyrin and 5.4 and 6.0 for deuteroporphyrin). These porphyrins, as well as their dimethyl ester forms, are shown to incorporate as monomers into the hydrophobic bilayer of egg phosphatidylcholine small unilamellar vesicles, although the esterified forms are highly aggregated in aqueous solutions. In the case of the non-esterified forms, the incorporation of the porphyrins into the lipidic bilayer is reversible and strongly pH-dependent. A theoretical model is presented which takes into account the various protonation steps and the partition equilibria of the porphyrin between the vesicle lipidic phase and the water medium. The neutral form of the porphyrin (i.e., carboxylic groups protonated) presents the higher affinity, with constants of $K \approx 2 \cdot 10^5$ and $K \approx 6 \cdot 10^6$ M^{-1} (relative to lipid concentration) for hematoporphyrin and deuteroporphyrin, respectively. Protonation of one inner nitrogen leading to the monocationic form is sufficient to prevent incorporation into the hydrophobic bilayer. On the other hand, deprotonation of the peripheral propionic chains leading to anionic forms is less effective. These interactions between vesicles and porphyrins lead to shifts of the apparent pK of nitrogens and carboxylic groups, the latter one being now in the range of physiological pH. These results are discussed with regards to the hypothesis of a possible role of pH in the preferential uptake of porphyrins by tumors.

Introduction

The preferential retention of porphyrins by tumors has led to the development of new methods of diagnosis and therapy based on the fluorescence and the photosensitizing properties of these molecules [1–3]. Cellular specificity [4] as well as extracellular tumor characteristics [5] including inadequate lymphatic drainage [6] or anomalous acid-base status [7–9] have been suggested to be responsible for the specific uptake of porphyrins by malignant tissues. Membrane structures appear to be the major targets of the photodynamic processes [10–12]. Photobiological damages on cytoplasmic [11], mitochondrial [13,14] and lysosomal [15] membranes have been reported. Incorporation into cultured cells and subsequent photoinactivation were found to drastically depend on porphyrin hydrophobicity [11,12,16]. The importance of the cellular partition of endogeneous

porphyrins which are accumulated in some diseases (porphyria) has also been emphasized [17]. Thus, the photobiological activity of porphyrins appears to be mainly governed by their ability to locate in the plasmic membrane or to cross it and reach intracellular targets.

Liposomes provide reproducible model systems allowing easy studies of porphyrin incorporation into lipid bilayer structures by means of spectroscopic techniques. Porphyrin-photosensitized processes in multilamellar liposomes have been reported by Grossweiner and co-workers [18–21]. Margalit and Cohen examined partition of hematoporphyrin and hematoporphyrin derivative into liposomes and reported that porphyrins are bound to large unilamellar vesicles as monomers [22]. Transport of porphyrins using liposomes also appears as a promising way for preferential delivery of the photosensitizer to tumor or to cell membrane structures [23,24].

In the present paper, we report on a spectrofluorimetric study of the incorporation of various porphyrins into egg phosphatidylcholine small unilamellar vesicles. The partition of dicarboxylic porphyrins between the aqueous phase and the lipidic bilayer is found to be strongly pH-dependent, the neutral form incorporating the best. These results are discussed with regards to possible uptake mechanisms of porphyrins by tumors.

Materials and Methods

Materials. Hematoporphyrin IX dimethyl ester and deuteroporphyrin IX dimethyl ester were purchased from Midcentury (U.S.A.). They were found to move as single spot on thin-layer chromatographic plates and were used as received. Hematoporphyrin IX was purified according to Vever-Bizet et al. [25]. Deuteroporphyrin IX was prepared from ferrideuteroporphyrin IX by removal of iron. The crude material was chromatographed on silica gel using a mixture of acetone/ethyl acetate/0.03 M hydrochloric acid (5 : 4 : 1.5, v/v) as eluent solution. Fresh porphyrin stock solutions were prepared in twice-distilled tetrahydrofuran. The structures of the porphyrins used are shown in Fig. 1.

Preparation of the vesicles. Small unilamellar vesicles of egg phosphatidylcholine (Sigma, type VIIE) were prepared by sonication of a suspension of the phospholipids in solutions comprising sodium phosphate (20 mM)/sodium phthalate (20 mM)/NaCl (0.15 M). This medium allows buffering conditions in the range pH 2–11 without significant changes in the ionic strength. Sonication was performed under nitrogen using a Branson sonifier (Model B15) equipped with a microtip probe set at 30% of duty cycle. The power output was approx. 60 W. Clear solutions were obtained after 15–20 min sonication. The stock solution of phospholipids was labelled with [^{3}H]phosphatidylcholine in order to determine precise concentrations of phospholipid vesicles solutions. The stock vesicle solution was diluted to the appropriate lipid concentration, adjusted to the desired pH and allowed to stand for at least 2 h before porphyrin addition. Stock porphyrin solutions (usually $4 \cdot 10^{-6}$ M) were prepared in tetrahydrofuran. Usually, 5 μl of these solutions were thoroughly mixed with 2 ml of buffer solutions containing preformed vesicles, and the system allowed to stand for 10 min at 20°C before

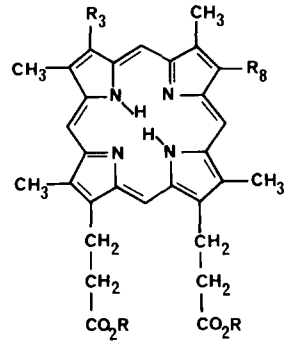

Porphyrin	R_3 , R_8	R
HP	$CHOHCH_3$	H
DP	H	H
HPDME	$CHOHCH_3$	CH_3
DPDME	H	CH_3

Fig. 1. Structure of porphyrins used. HP, hematoporphyrin; DP, deuteroporphyrin; HPDME, hematoporphyrin dimethyl ester; DPDME, deuteroporphyrin dimethyl ester.

fluorescence measurements were carried out. The addition of such minimal amounts of tetrahydrofuran did not affect the vesicles. The final porphyrin concentration was usually $1 \cdot 10^{-8}$ M.

Fluorescence measurements. Fluorescence emission spectra were recorded using an Aminco SPF 500 spectrofluorimeter. Excitation was usually set at 400 nm with slits giving a band of 4 nm half-width. All spectroscopic measurements were carried out at 20°C. Fitting of the titration curves were performed using a Hewlett-Packard computer model 9816S.

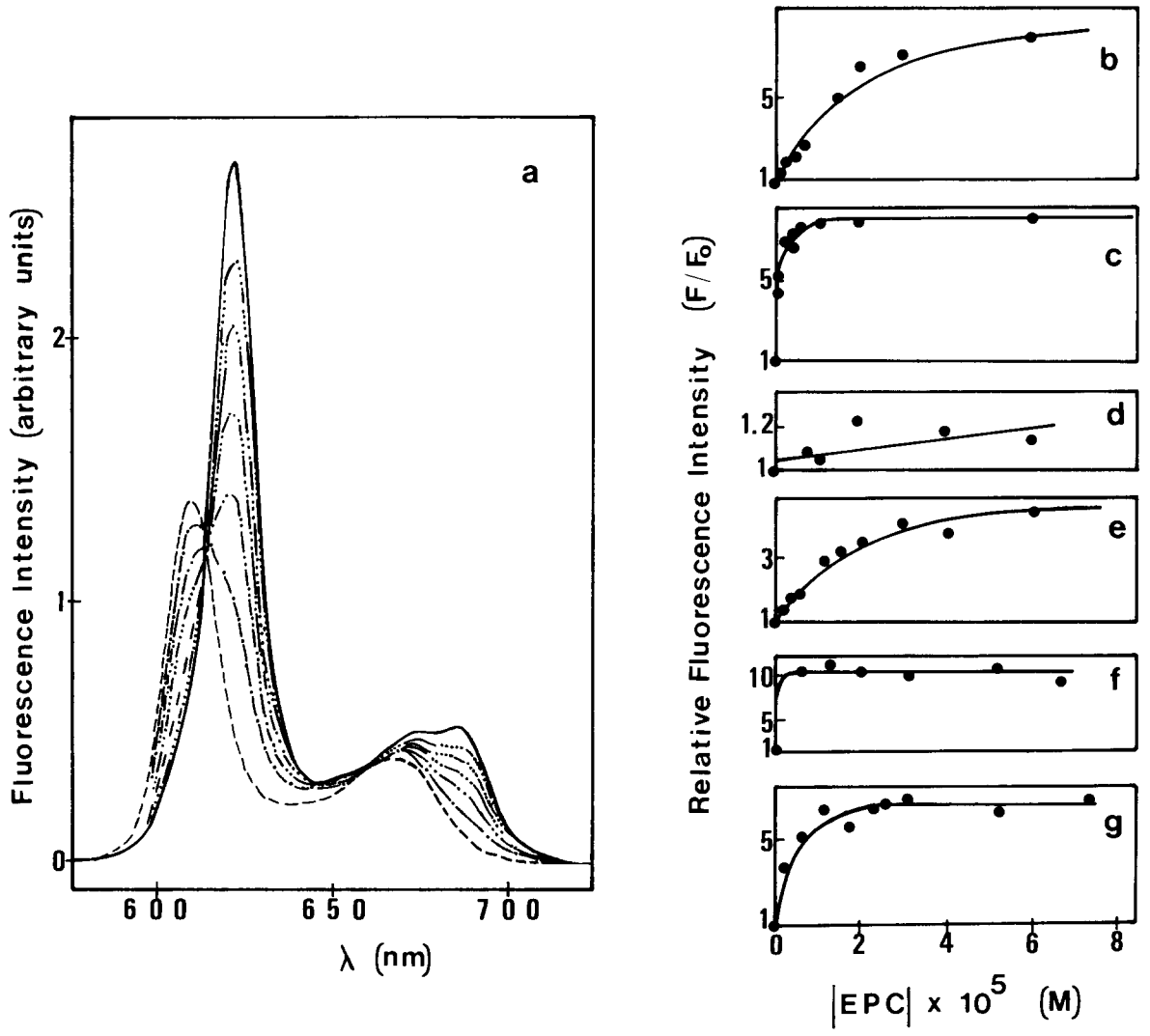

Fig. 2. Interaction of porphyrins with vesicles at constant pH. (a) Emission fluorescence spectra evolution upon addition of vesicles to deuteroporphyrin ($1 \cdot 10^{-8}$ M) buffered solutions (pH 7.2). Lipid concentrations were: – – –, zero; – · – · –, $4.9 \cdot 10^{-6}$; – · · – · · –, $9.7 \cdot 10^{-6}$; – · · · · –, $1.65 \cdot 10^{-5}$; – · · · · · –, $2.43 \cdot 10^{-5}$; – · · · · · · –, $3.40 \cdot 10^{-5}$; and ———, $4.37 \cdot 10^{-5}$ M. (b–g) Dependence of the relative emission fluorescence intensity on lipid concentration: b, deuteroporphyrin, pH 7.2; c, deuteroporphyrin, pH 5.07; d, hematoporphyrin, pH 7.2; e, hematoporphyrin, pH 5.07; f, deuteroporphyrin dimethyl ester, pH 7.2; g, hematoporphyrin dimethyl ester, pH 7.2.

Results

Porphyrin incorporation into egg phosphatidylcholine vesicles at constant pH

Before dealing with systems involving liposomes, the solution behavior of porphyrins was examined. In tetrahydrofuran, the porphyrin exhibited absorption and emission spectra characteristic of monomeric forms over a wide range of concentrations. Fluorescence maxima were found at 625 and 692 nm with apparent vibrational structures at 655 and 675 nm for hematoporphyrin and 622 and 689 nm with structures at 652 and 675 nm for deuteroporphyrin. The excitation spectra were found to match quite well the absorption spectra. The emission and excitation fluorescence spectra of hematoporphyrin dimethyl ester and deuteroporphyrin dimethyl ester were found to be very similar to those of the parent porphyrins. Addition of the stock porphyrin solutions in tetrahydrofuran to the buffer solution (pH 7.2) containing no liposomes resulted in quite different behaviors according to the porphyrin structure. The free dicarboxylic porphyrins at a final concentration of $1 \cdot 10^{-8}$ M gave solutions presenting the intense fluorescence spectra expected for monomeric species in aqueous solutions (λ emission = 615 and 674 nm for hematoporphyrin, 612 and 671 nm for deuteroporphyrin with no apparent structure). On the other hand, the porphyrin ester forms yielded solutions with weak fluorescence emission. The fluorescence intensity was found to somewhat depend on the conditions the solutions were prepared. These findings suggested quite unreliable formation of large aggregates of these hydrophobic molecules in water medium. Also, the porphyrins were found to adsorb on the glass vessel used to make solutions. To determine the amount of porphyrin adsorbed, the vessel was washed with tetrahydrofuran and the concentration of the porphyrin extracted was measured by fluorescence using calibration curves.

The gradual addition of preformed vesicles to deuteroporphyrin solutions at pH 7.2 led to the spectral changes depicted in Fig. 2a. The presence of isoemissive points can be noted. The shift of the main fluorescence peak from 612 to 623 nm suggests that the porphyrin moves from an aqueous to a lipidic environment (see above, the spectral data reported for aqueous and tetrahydrofuran solutions as references). A good reversibility was observed when the vesicle concentration was progressively decreased by adding a porphyrin solution to a solution of preformed vesicles. In all instances, the partition was found to proceed within less than 10 min and no significant further changes in fluorescence spectra took place over hours. No changes in the porphyrin partition between the lipidic and aqueous phases were observed when solutions were sonicated again. All these data are consistent with simple reversible partition of the porphyrin between the bulk aqueous phase and the lipidic bilayer of the vesicles. The fluorescence changes at a wavelength corresponding to the porphyrin embedded in the vesicles are represented in Fig. 2b in terms of F/F_0 vs. [lipid] where F and F_0 stand for the intensities of fluorescence presented by solutions containing vesicles or not, respectively. As discussed below, reference to the lipid concentration rather than to the vesicle concentration is made. Similar results were obtained with solutions at pH 5.07 but, in this case, the partition was much more in favor of the vesicles. This pH effect is well-exemplified by curves shown in Fig. 2b and c. The incorporation of hematoporphyrin into the vesicles was a much less favored process but it also depended on pH, as shown in Fig. 2d and e. At pH 7.2, almost no incorporation occurred even at the highest lipid concentrations. The fluorescence emission maximum of hematoporphyrin incorporated into vesicles was at 623 nm.

The incorporation of the dimethyl ester forms was investigated in a similar way, but in this case, the incubation was pursued overnight. Even in the presence of liposomes, the porphyrins were found to adsorb on glass vessel. The amount of adsorbed porphyrin, which was less important at higher vesicle concentration, was determined as abovementioned. The actual porphyrin concentrations and corrected fluorescence intensities were calculated accordingly. As shown in Fig. 2f and g, the ester forms readily incorporate at pH 7.2. The dimethyl ester and the free acid forms presented very similar emission spectra when incorporated.

The pH dependence of porphyrin incorporation into vesicles exemplified in Fig. 2 prompted us to study the acid-base properties of the dicarboxylic porphyrins in absence and in presence of vesicles.

Spectrofluorimetric porphyrin titration in absence of vesicles

Fig. 3 displays typical sets of fluorescence emission spectra recorded on acid-base titration of hematoporphyrin dissolved in phosphate/phthalate buffer solutions containing NaCl (0.15 M) to keep ionic strength constant. The fluorescence emission spectrum of hematoporphyrin around pH 4 was characterized by quite broad bands at 607 and 654 nm. Decreasing the pH from about 4 to 1 leads to an increase of the fluorescence emission with the appearance of peaks at 596 and 652 nm. On the other hand, build up of sharp emission peaks at 615 and 674 nm was observed when the pH was increased. No other changes were observed above pH 7.25. A similar behavior was observed on titration of deuteroporphyrin. Solutions at pH 5 were found to present broad emission bands at 612 and 660 nm. When the pH was decreased from 5 to 1.2, sharp bands at 593 and 550 nm grew up. Gradual build up of bands at 612 and 671 nm was observed in the alkaline region. Titration curves at the most significant wavelengths are given in Figs. 4a and 5a for hematoporphyrin and deuteroporphyrin, respectively.

Spectrofluorimetric porphyrin titration in the presence of vesicles

The stability of the vesicles in the range of pH to be investigated was considered first. In Fig.4b, is shown the pH dependence of the intensity of light scattered by egg phosphatidylcholine vesicle solutions. It appears fairly constant in a wide pH range, suggesting that the vesicles remain unchanged between pH 2 and 10. Vesicle fusion at the extreme pH can account for the observed increase in scattering.

A typical set of fluorescence emission spectra recorded on titration of hematoporphyrin solutions in phosphate/phthalate buffer containing egg phosphatidylcholine vesicles ([Lipid] = 6.6 ·

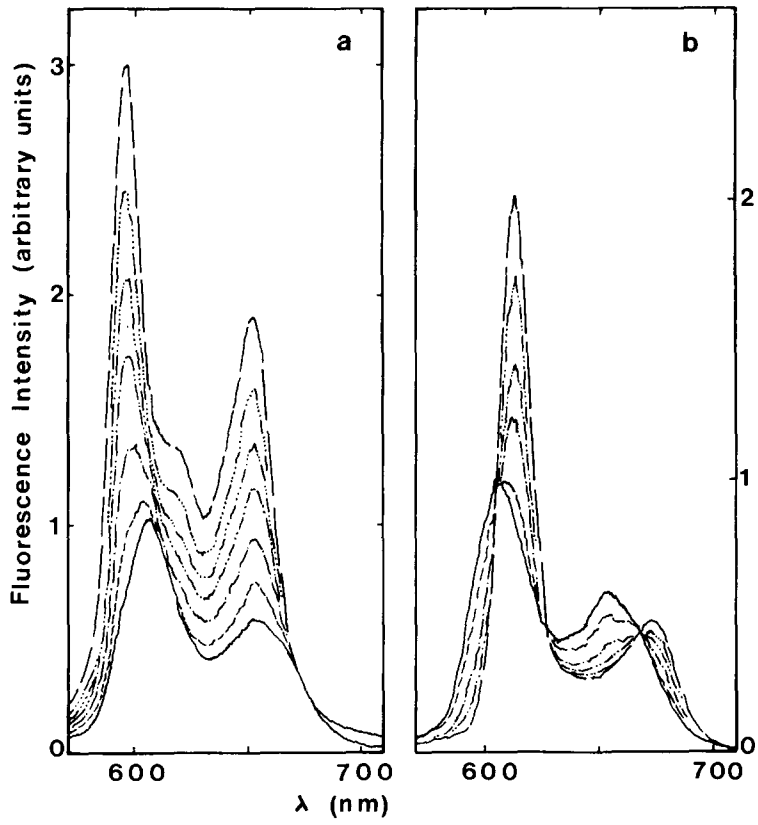

Fig. 3. pH dependence of emission fluorescence spectra of hematoporphyrin. pH values were: (a) ———, 4.33; – – –, 3.95; – · –, 3.53; – · · –, 3.18; – · · · –, 2.83; – · · · · –, 2.42; — —, 1.15. (b) ———, 4.33; – – –, 4.63; – · –, 5.0; – · · –, 5.25; – · · · –, 5.64; — —, 7.25–11.3.

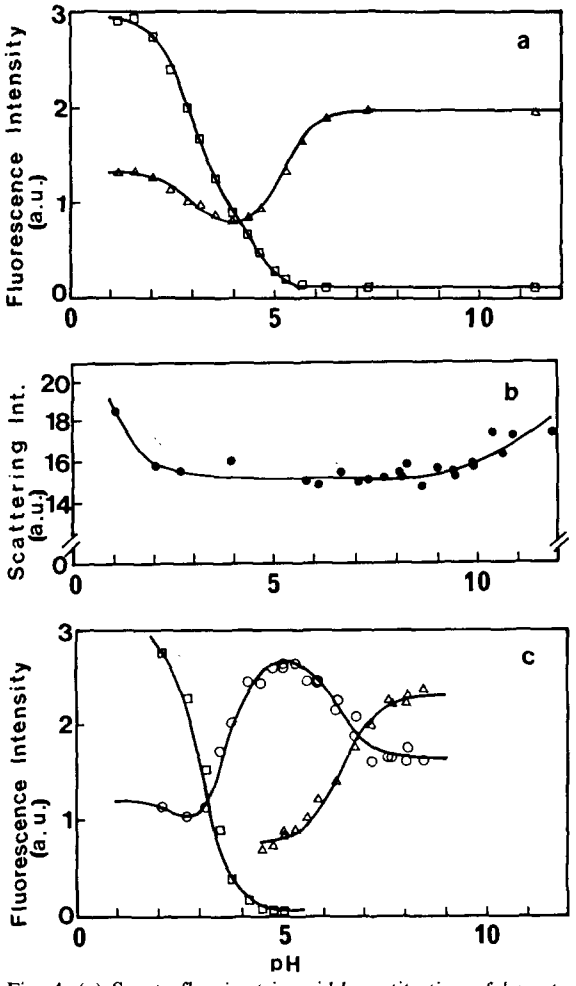

Fig. 4. (a) Spectrofluorimetric acid-base titration of hematoporphyrin ($1 \cdot 10^{-8}$ M) at various wavelengths: (□) 596 nm; (△) 615 nm. The full line corresponds to the theoretical curve (see text). (b) pH dependence of the intensity of light scattered by vesicle solutions. The lipid concentration was $5.6 \cdot 10^{-5}$ M. (c) Spectrofluorimetric acid-base titration of hematoporphyrin ($1 \cdot 10^{-8}$ M) in the presence of vesicles ([lipid] = $6.6 \cdot 10^{-5}$ M) at various wavelengths: (□) 596 nm; (△) 615 nm; (○) 623 nm. The full line corresponds to the theoretical titration curve (see text).

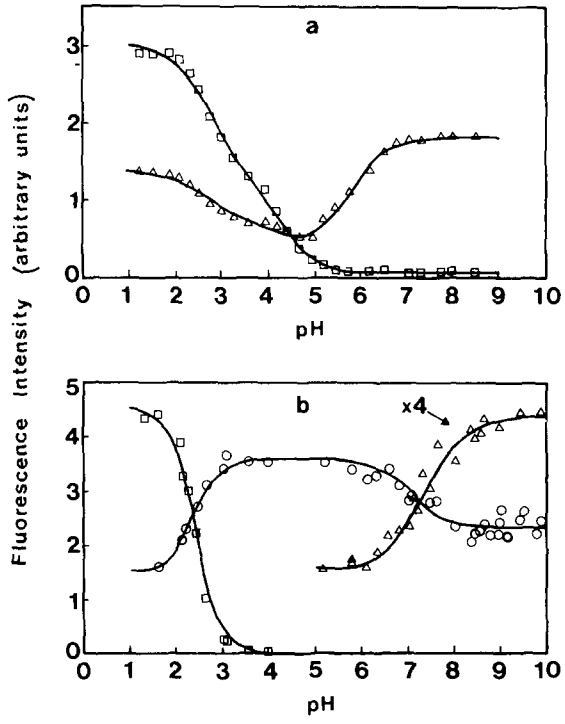

Fig. 5. (a) Spectrofluorimetric acid-base titration of deuteroporphyrin ($1 \cdot 10^{-8}$ M) at various wavelengths; (□) 593 nm; (△) 612 nm. The full line corresponds to the theoretical titration curve (see text). (b) Spectrofluorimetric acid-base titration of deuteroporphyrin ($1 \cdot 10^{-8}$ M) in the presence of vesicles ([lipid] = $5.6 \cdot 10^{-5}$ M) at various wavelengths: (□) 593 nm; (△) 612 nm; (○) 623 nm.

10^{-5} M) is shown in Fig. 6. It displays interesting features as compared to the one depicted in Fig. 3. The spectrum with broad bands at 607 and 654 nm presented by solutions around pH 4 is no more observed. On the other hand, a new spectrum characterized by well-resolved fluorescence peaks at 623 and 687 nm is found around pH 4–6. This spectrum was assigned to the porphyrin embedded in the lipidc phase of the vesicles (see Discussion). The fluorescence spectra presented by either alkaline (pH > 8) or very acidic (pH < 2) solutions were found to be independent of the presence of vesicles (compare Figs. 3 and 6), suggesting that the corresponding forms of the porphyrin have very low affinity for the vesicles. In Fig. 4c are shown titration curves at the wavelengths characteristic of the various species: 596 nm (acidic form), 623 nm (incorporated form), 615 nm (alkaline form). It is noteworthy that, in the presence of the vesicles, the titration curves corresponding to the formation of the acidic and alkaline forms are respectively shifted to extreme pH. The shape of the curves is also affected.

Fluorescence spectra of deuteroporphyrin solutions containing vesicles ([Lipid] = $5.6 \cdot 10^{-5}$ M) are reported in Fig. 7 for typical pH values. As for hematoporphyrin, a new spectrum characterized

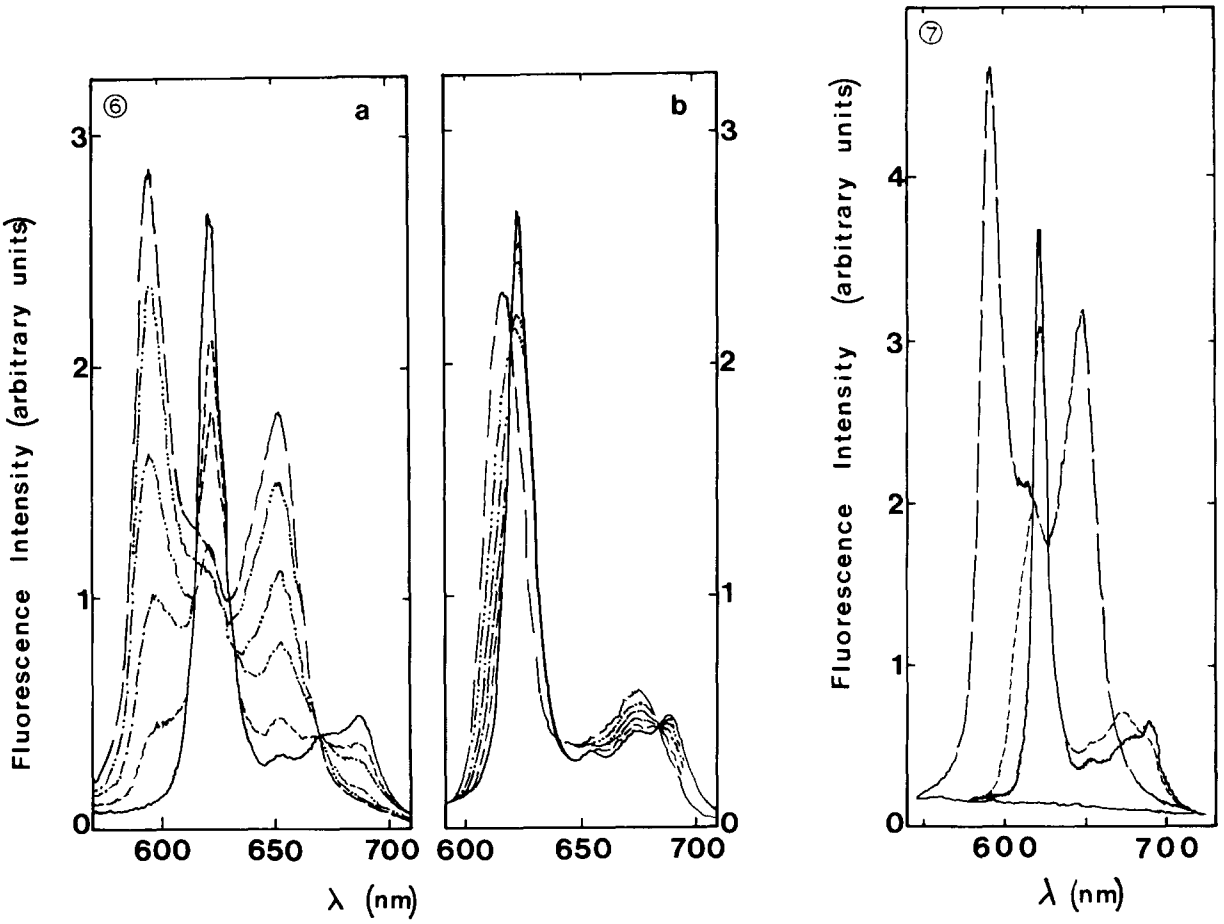

Fig. 6. pH dependence of emission fluorescence spectra of hematoporphyrin ($1 \cdot 10^{-8}$ M) in the presence of vesicles ([lipid] = $6.6 \cdot 10^{-5}$ M). pH values were: (a) ———, 4.80; – – –, 3.80; –·–, 3.50; –··–, 3.18; –···–, 2.73; — —, 2.10. (b) ———, 4.80; – – –, 5.62; –·–, 5.90; –··–, 6.33; –···–, 6.81; — —, 8.05.

Fig. 7. pH dependence of emission fluorescence spectra of deuteroporphyrin ($1 \cdot 10^{-8}$ M) in the presence of vesicles ([lipid] = $5.6 \cdot 10^{-5}$ M). pH values were: — —, 1.6; ———, 5.15; – – –, 9.52.

by sharp bands at 623 and 690 nm was displayed by solutions around pH 5. Also, a spectrum identical to the one presented by vesicle-free solutions was obtained at acidic pH. On the other hand, in the alkaline region, even at the highest pH, it was impossible to recover the spectrum presented by vesicle-free solutions. The spectrum reported in Fig. 7 for a solution at pH 9.5 displays only small decrease and increase of the 612 and 623 nm bands, respectively. This indicates that deuteroporphyrin still interacts with the vesicles in alkaline conditions. Titration curves at wavelengths characteristic of the three species (593, 623 and 612 nm for the acidic, incorporated and alkaline forms, respectively) are reported in Fig. 5b. As mentioned before in the case of hematoporphyrin, the shifts towards extreme pH of the titration curves illustrate the strong effect of the vesicles on the pattern of porphyrin distribution between the various neutral, anionic or cationic forms. In the same way, the titration curve shapes are significantly modified.

Discussion

Porphyrins in aqueous solutions

The solution structure of dicarboxylic porphyrins is essentially governed by aggregation and acid-base processes. The aggregation of hematoporphyrin and deuteroporphyrin in aqueous buffered saline solutions (pH 7.2) has been investigated by Margalit et al. using fluorimetric techniques [26,27]. In dilute solutions (10^{-8}–10^{-6} M), dimerization was found to be the dominant aggregation process. The values determined for the dimerization equilibrium constants were $4 \cdot 10^5$ and $2.3 \cdot 10^6$ M^{-1} at 25°C for hematoporphyrin and deuteroporphyrin, respectively. It can be calculated that in neutral solutions containing a total porphyrin concentration of $1 \cdot 10^{-8}$ M, i.e., under the conditions of the present study, only 0.8 and 4.2% of hematoporphyrin and deuteroporphyrin are dimerized, respectively. Although these values may increase at lower pH, aggregation processes are not believed to interfere greatly with equilibria to be discussed below. Obviously, this is not true for the ester forms of the porphyrins, which largely aggregate, as shown by the weak fluorescence of their aqueous solutions.

Dicarboxylic porphyrins possess two acidic and two basic groups undergoing protonations in the pH range 1–8 [28]. In Fig. 1 is depicted the structure of the neutral form PH_2 (carboxylic groups protonated, i.e., R = H). It is the predominant form around pH 4–5 and is characterized by broad fluorescence emission peaks (as noted below, in the case of hematoporphyrin, a zwitterion form could also be present in this pH range). At higher pH, the two propionic acid chains successively deprotonate, leading to the monoanionic (PH^-) and the dianionic (P^{2-}) forms which exhibit stronger fluorescence emission (a simplified notation is used here: the anionic forms to be discussed are not related with species formed on deprotonation of the porphyrin pyrrole nitrogen which are observed at much higher pH). In the acidic range, two protons can be added successively on the imine-type nitrogen atoms (–N=) of the porphyrin ring to form the monocation (PH_3^+) and the dication (PH_4^{2+}). These species have been characterized in organic [29] or micelle [28] solutions where well-resolved successive protonations are observed. In the visible region, the monocationic and dicationic forms present three and two absorption bands, respectively [29]. The low-energy absorption bands of these species do not greatly differ in their wavelengths, but they are shifted to the blue as compared to the one of the neutral form. The fluorescence emission changes reported in Fig. 3a, are thus in agreement with the formation of cationic species. They are characterized by peaks at 596 and 593 nm for hematoporphyrin and deuteroporphyrin, respectively. Successive protonations are evidenced by shoulders on the titration curves shown in Figs. 4a and 5a. The upper line in Scheme I summarizes these various protonation steps.

$$\begin{array}{ccccccc} PH_4^{2+} & \overset{K_{N2}}{\rightleftarrows} & PH_3^+ & \overset{K_{N1}}{\rightleftarrows} & PH_2 & \overset{K_{A1}}{\rightleftarrows} PH^- & \overset{K_{A2}}{\rightleftarrows} P^{2-} \\ & & K_2 \downarrow \uparrow & & K_1 \downarrow \uparrow & K \downarrow \uparrow & \\ & & PH_2L & \rightleftarrows & (PHL)^- & \rightleftarrows & (PL)^{2-} \end{array}$$

Scheme I

Dissociation constants are defined as:

$$K_{A1} = \frac{[PH^-][H^+]}{[PH_2]} \tag{1a}$$

$$K_{A2} = \frac{[P^{2-}][H^+]}{[PH^-]} \tag{1b}$$

$$K_{N1} = \frac{[PH_2][H^+]}{[PH_3^+]} \tag{1c}$$

$$K_{N2} = \frac{[PH_3^+][H^+]}{[PH_4^{2+}]} \tag{1d}$$

Let us define C as the total porphyrin concentration:

$$C = [PH_4^{2+}] + [PH_3^+] + [PH_2] + [PH^-] + [P^{2-}] \tag{2}$$

and

$$\alpha = 1 + \frac{[H^+]}{K_{N1}} + \frac{[H^+]^2}{K_{N1} \cdot K_{N2}} + \frac{K_{A1}}{[H^+]} + \frac{K_{A1} \cdot K_{A2}}{[H^+]^2} \tag{3}$$

it follows:

$$C = \alpha[PH_2]$$

A quantitative analysis of titration curves shown

in Figs. 4a and 5a is possible if, firstly, the fluorescence emitted by each form at a given wavelength is directly proportional to its concentration (via proportionality factors hereafter noted as f) and secondly, the fluorescence of a solution is equal to the sum of the fluorescence contributions of the various species present. These conditions are obeyed [30] with the very weakly absorbing solutions used in the present study. A last assumption appears to be fulfilled owing to the fluorescence lifetime of porphyrins (5–15 ns, [31]): the excited state giving rise to the fluorescence emission does not undergo acid-base reactions during its lifetime. In order to simplify further the mathematical approach, we also define (for the sake of simplifying typography, the charges of the various species will be hereafter omitted in the notations of proportionality factors):

$$\alpha' = f_{PH2} + f_{PH3}\frac{[H^+]}{K_{N1}} + f_{PH4}\frac{[H^+]^2}{K_{N1}\cdot K_{N2}} + f_{PH}\frac{K_{A1}}{[H^+]} + f_P\frac{K_{A1}\cdot K_{A2}}{[H^+]^2} \quad (5)$$

It is easily shown that:

$$F = \alpha'[PH_2] \quad (6)$$

or

$$F = \frac{\alpha'}{\alpha}C \quad (7)$$

where F is the total fluorescence intensity presented by a porphyrin solution at a given pH. Computer simulations of the dependence of the fluorescence according to the pH using Eqn. 7 were performed. The values of the various dissociation constants and proportionality parameters were varied until the best fit of experimental points was obtained. The accuracies on the values of dissociation constants and proportionality factors are related. However, it must be pointed out that some of the latter parameters can be independently determined with a good accuracy. For instance, f_{PH4} and f_P can be obtained from fluorescence measurements at low and high pH, respectively. Other values (f_{PH3}, f_{PH2}) can be reasonably estimated from experimental data. The unresolved successive dissociations of propionic groups led to more uncertainty. In our calculations, we assumed that $f_{PH} = (f_{PH2} + f_P)/2$. Best theoretical fitting curves are shown in Figs. 4a and 5a as full lines. The corresponding values for the pK of the ionisable groups are given in Table I. They are in agreement with those extrapolated from studies in other media and from pK of related substances [28]. The pK of the two propionic chains differ by about 0.5 unit, likely due to electrostatic effects and are slightly higher than the pK of propionic acid. It is noted that hematoporphyrin may partly exist as a zwitterion around pH 4.8 in aqueous solutions.

Interactions of porphyrins with vesicles

The fluorescence results on neutral aqueous solutions containing vesicles and the ester forms of hematoporphyrin and deuteroporphyrin provide large evidences for the incorporation of the non-charged form of these molecules into the lipidic bilayer. Indeed, at pH 7.2, no protonation of the inner nitrogens is expected and esterification suppresses the possibility of propionic chain ionization. As a matter of fact, the fluorescence spectra of these molecules, either interacting with vesicles or dissolved in organic solvent, are very similar. As expected for these highly hydrophobic molecules, their partition between the aqueous phase and the lipidic bilayer is much more in favor of the latter environment. It should be re-

TABLE I

VALUES OF pK AND EQUILIBRIUM CONSTANTS AS SHOWN IN SCHEME I FOR HEMATOPORPHYRIN AND DEUTEROPORPHYRIN

	pK_{N2}	pK_{N1}	pK_{A1}	pK_{A2}	K_2 (M^{-1})	K_1 (M^{-1})	K (M^{-1})
Hematoporphyrin	2.9 ± 0.1	4.7 ± 0.1	4.95 ± 0.15	5.45 ± 0.15	$\approx 2\cdot10^5$	$\approx 1\cdot10^5$	$\leqslant 10^3$
Deuteroporphyrin	2.7 ± 0.1	4.4 ± 0.1	5.4 ± 0.2	6.0 ± 0.2	$\approx 6\cdot10^6$	$\approx 2\cdot10^6$	$\approx 1\cdot10^5$

minded that aggregates have been suggested to play an important role in porphyrin uptake by tumors [32]. The present system provides an interesting example of incorporation into lipidic structures of porphyrins highly aggregated in solution. Further kinetic or thermodynamic analysis of these systems are however precluded by the complexity of the aggregation processes.

In contrast to their ester forms, hematoporphyrin and deuteroporphyrin are well-characterized in aqueous solutions. The reversibility of the partition of these porphyrins between the bulk aqueous phase and the vesicle phase was pointed out in the results. In addition, the lack of effect of sonication vesicle solutions already incubated with porphyrins and the rapidity of the partition process largely demonstrate that thermodynamic equilibrium conditions are attained. The extended scheme shown above which includes equilibria between porphyrins and vesicles is based on this premise and on the following observations. The fluorescence spectra of hematoporphyrin or deuteroporphyrin below pH = 2 do not depend on the presence of vesicles, indicating that the cationic forms do not incorporate into the lipidic bilayer. On the other hand, although neutral forms are best incorporated, negative charges on the propionic side-chains do not totally impede incorporation. Thus, even at the highest pH, interactions between vesicles and deuteroporphyrin are observed. A further assumption will be made: the incorporation of a porphyrin molecule is independent of the presence of another porphyrin molecule in a vesicle. Assuming a mean number of 3000 lipid molecules per vesicle, the mean ratio between the number of porphyrin molecules incorporated and the number of vesicles is calculated to be less than 0.5 for most experiments and does not exceed a few dozen in the less favorable cases. Furthermore, the sharp fluorescence spectrum of embedded porphyrin molecules strongly suggests that they are monomeric. So, either a vesicle contains no more than one porphyrin molecule or if several molecules are incorporated they are remote enough so that they do not interact. Consequently, we will refer hereafter to the lipid concentration rather than to the vesicle concentration estimated from their mean size. The various equilibria involved in porphyrin-vesicle systems are summarized in Scheme I. The affinity constants of the various forms of the porphyrin for the vesicles are defined by:

$$K_2 = \frac{[PH_2L]}{[PH_2][L]} \tag{8a}$$

$$K_1 = \frac{[(PHL)^-]}{[PH^-][L]} \tag{8b}$$

$$K = \frac{[(PL)^{2-}]}{[P^{2-}][L]} \tag{8c}$$

where [L] refers to the lipid concentration and PH_2L, $(PHL)^-$ and $(PL)^{2-}$ represent the incorporated neutral, monoanionic and dianionic forms, respectively.

In the same way as above we will define:

$$\beta = K_2 + \frac{K_1 \cdot K_{A1}}{[H^+]} + \frac{K \cdot K_{A1} \cdot K_{A2}}{[H^+]^2} \tag{9}$$

$$\beta' = f_{PH2L} \cdot K_2 + f_{PHL} \frac{K_1 \cdot K_{A1}}{[H^+]} + f_{PL} \frac{K \cdot K_{A1} \cdot K_{A2}}{[H^+]^2} \tag{10}$$

The total porphyrin concentration:

$$C = [PH_4^{2+}] + [PH_3^+] + [PH_2] + [PH^-] + [P^{2-}] + [PH_2L] + [(PHL)^-] + [(PL)^{2-}] \tag{11}$$

can now be expressed by:

$$C = (\alpha + \beta[L])[PH_2] \tag{12}$$

The fluorescence of a solution is given by:

$$F = (\alpha' + \beta'[L])[PH_2] \tag{13}$$

or

$$F = \frac{\alpha' + \beta'[L]}{\alpha + \beta[L]} C \tag{14}$$

Denoting F_0 and F_∞ the fluorescence of solutions containing no and sufficient amount of vesicles to displace equilibria toward complete porphyrin incorporation, respectively, it can be shown [33]

that:

$$F - F_0 = \frac{\alpha\beta' - \alpha'\beta}{\alpha(\alpha + \beta[\mathrm{L}])}[\mathrm{L}]C \tag{15}$$

$$F_\infty - F = \frac{\alpha\beta' - \alpha'\beta}{\beta(\alpha + \beta[\mathrm{L}])}C \tag{16}$$

and

$$\frac{F - F_0}{F_\infty - F} = \frac{\beta}{\alpha}[\mathrm{L}] \tag{17}$$

or

$$\log\frac{F - F_0}{F_\infty - F} = \log\frac{\beta}{\alpha} + \log[\mathrm{L}] \tag{18}$$

Relation 17 can be modified to:

$$\frac{1}{F - F_0} = \frac{1}{F_\infty - F_0} + \frac{1}{F_\infty - F_0} \times \frac{\alpha}{\beta} \times \frac{1}{[\mathrm{L}]} \tag{19}$$

When the pH is maintained constant so are α, α', β and β'. As a consequence, if [L] is varied, this complex system behaves as it would involve a simple equilibrium [33] of the type A + B $\rightleftharpoons$ AB. But, now, β/α represents an apparent equilibrium constant, K_{app}, the value of which depends on pH. From Eqn. 15, an important conclusion can be derived which applies when the pH and the porphyrin concentration are constant. The intersection of any intermediate spectrum ([L] $\neq$ 0) with the initial one must correspond to an isoemissive point. Indeed, this implies that $\alpha\beta' - \alpha'\beta \equiv 0$ which must apply to any other value of [L]. The set of spectra reported in Fig. 2a shows good agreement with this conclusion.

The validity of Scheme I can be verified by plotting $1/(F - F_0)$ vs. $1/[\mathrm{L}]$ or $\log(F - F_0)/(F_\infty - F)$ vs. log[L]. The former representation is useful when F_∞ cannot be attained experimentally. In this case, its value is obtained through extrapolation. In Fig. 8, are reported data on the interaction of deuteroporphyrin with vesicles according to the second representation. In agreement with Eqn. 18, data from two experiments performed at various pH are fitted by straight lines with slopes near unity. As expected, however, their positions along the abscissa, which is equal to $-\log K_{app}$, are pH-dependent.

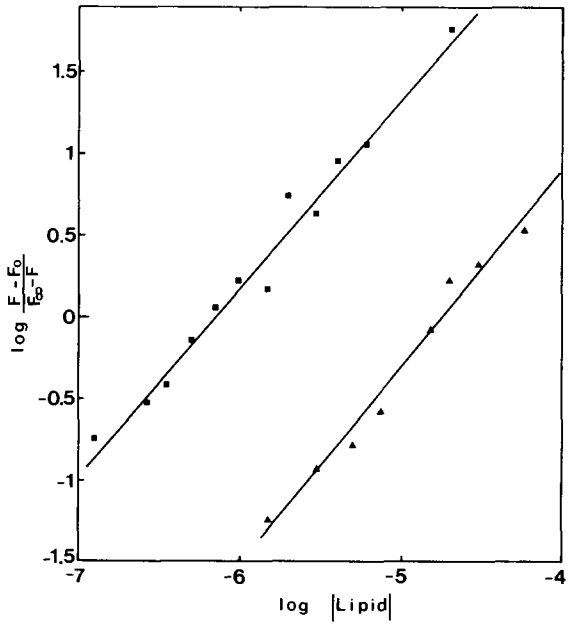

Fig. 8. Interaction of deuteroporphyrin with vesicles. Plot according to Eqn. 18. pH was: ■, 5.07; ▲, 7.20. Slopes as derived from least-mean-square analysis were found to be 1.14 and 1.18, respectively.

The theoretical fluorescence changes expected from acid titration of mixed systems containing porphyrins and vesicles can be computed according to Eqn. 14 assuming values for f_{PH2L}, f_{PHL}, f_{PL}, K_2, K_1 and K, and using the pK and other f values previously determined. Best fits, which are shown in Figs. 4c and 5b as full lines, were obtained with the equilibrium constant values reported in Table I and assuming $f_{PH2L} = f_{PHL}$. In the case of deuteroporphyrin, which interacts with vesicles even when its two propionic chains are deprotonated, f_{PL} at 623 nm (emission peak of the incorporated form) was found to be smaller than f_{PH2L} or f_{PHL}. An upper limit of the affinity constant of fully deprotonated hematoporphyrin for lipids is given. A more accurate value cannot be obtained owing to the limited lipid concentration experimentally accessible.

In view of these results, the interactions between porphyrins and vesicles can be described as follows. Dicarboxylic porphyrins are incorporated into vesicles with their hydrophobic core buried into the lipidic bilayer. As a matter of fact, as compared to deuteroporphyrin, hematoporphyrin

with polar alcoholic chains on the tetrapyrrolic nucleus, presents a lower affinity for vesicles (see Table I). In the same way, protonation of one inner nitrogen which drastically reduces the hydrophobicity of the porphyrin core impedes the incorporation into the vesicle bilayer. The effect of negative charges on the propionic chains is clearly evidenced by the relative values of the affinity constants, $K_2 > K_1 \gg K$. However, this effect appears much less drastic than protonation of the inner nitrogens, suggesting that the incorporated molecules have their propionic acid chains lying near the polar heads of the bilayer. The smaller value of f_{PL} as compared to f_{PH2L} or f_{PHL} may indicate that the dianionic form of deuteroporphyrin lies closer to the vesicle polar heads.

The relative affinities of the various forms of the porphyrins for the vesicles have interesting consequences on the acid-base titration curves of mixed systems as exemplified in Figs. 4c and 5b. It should be first pointed out that the pK which could be derived from these curves are apparent pK, the values of which depend on the various affinity constants and on the vesicle concentration. As expected from the drastic affinity decrease associated with the first nitrogen protonation, the corresponding apparent pK is shifted to a lower value. This results in an almost simultaneous titration of the two inner nitrogens. Likewise, the shift of the apparent pK of the propionic groups towards higher pH is the consequence of the relative affinities of the various forms with $K_2 > K_1 \gg K$. However, as anionic forms retain some affinity for the vesicles, the shape of the titration curve is less affected than in the previous case.

A model for the preferential uptake of porphyrins by tumors

The above results clearly show that pH largely governs the interactions of dicarboxylic porphyrins with membranes through acid-base equilibria involving ionizable groups. With regard to biological aspects, propionic chains appear particularly important. Indeed, as exemplifeid by our model system, owing to interactions with membranes, the apparent pK of these acidic groups can be shifted enough to attain physiological pH. The incorporation of the porphyrin as well as its distribution among the various forms, PH_2L, $(PHL)^-$ and $(PL)^{2-}$, drastically depend on pH. As exemplified in Figs. 4c, 5b and in a related paper [34], a small decrease in pH around 7 leads to the increase of the amount of incorporated porphyrin. Also, equilibria between the various incorporated species are shifted, resulting in an increased proportion of the neutral form PH_2L [34]. As the latter gives rise to little electrostatic interactions, it is expected to cross a membrane structure more rapidly than do charged forms. It is noteworthy that, in some instances, tumors have been shown to be more acidic by 0.2–0.4 pH units than normal tissues [7]. So, a lowered local pH could contribute to the preferential uptake of porphyrins by tumors. As a matter of fact, cells were found to be more sensitive to photoinactivation at low pH [8,9]. The same conclusion likely applies to hematoporphyrin derivative, the acid-base properties of which have been reported [35]. Indeed, hematoporphyrin derivative is composed of various porphyrins belonging to the class of dicarboxylic porphyrins [36]. It is noted, however, that the long-term retention of hematoporphyrin derivative, which is likely to be responsible for its therapeutic superiority, likely involves processes taking place after penetration of the drug into cells [37]. The comparison of hematoporphyrin with deuteroporphyrin also illustrates how minor changes in the nature of some side-chains can drastically affect the affinity of porphyrins for membranes.

Conclusion

The solution behavior of porphyrins in absence or in presence of egg phosphatidylcholine small unilamellar vesicles has been quantitatively described, as a function of pH, in terms of thermodynamical equilibria. The partition of the porphyrin between the bulk aqueous phase and the hydrophobic vesicle bilayer appears dominated by both the porphyrin structure and its charge which depends on pH. The highest affinities are presented by neutral forms. These physicochemical data give support to the hypothesis that pH may partly control the selective uptake of dicarboxylic porphyrins by tumors which are known to be more acidic than normal tissues.

Acknowledgments

This work was supported by grant MRI 83M0654 from the Ministère de la Recherche et de la Technologie and ATP GBM 6931 from CNRS. The authors are indebted to Professor C. Helene, Dr. M. Rougee and Professor G. Laustriat for helpful discussions, and to O. Delgado for porphyrin purification.

References

1 Kessel, D. and Dougherty, T.J. (1983) Porphyrin Photosensitization, Plenum Press, New York
2 Andreoni, A. and Cubeddu, R. (1984) Porphyrins in Tumor Phototherapy, Plenum Press, New York
3 Doiron, R.D. and Gomer, C.J. (1984) Porphyrin Localization and Treatment of Tumors, Alan R. Liss, New York
4 Andreoni, A., Cubeddu, R., De Silvestri, S., Laporta, R., Ambesi-Impiombato, F.S., Esposito, M., Mastrocinque, M. and Tramontano, D. (1983) Cancer Res. 43, 2076–2080
5 Moan, J., Steen, H.B., Feren, K. and Christensen, T. (1981) Cancer Lett. 14, 291–296
6 Bugelski, P.J., Porter, C.W. and Dougherty, T.J. (1981) Cancer Res. 41, 4602–4612
7 Gullino, P.M., Grantham, F.H., Smith, S.H. and Haggerty, A.C. (1965) J. Natl. Cancer Inst. 34, 857–869
8 Moan, J., Smedshammer, L. and Christensen, T. (1980) Cancer Lett. 9, 327–332
9 Moan, J. and Christensen, T. (1981) Photobiochem. Photobiophys. 2, 291–299
10 Volden, G., Christensen, T. and Moan, J. (1981) Photobiochem. Photobiophys. 3, 105–111
11 Kessel, D. (1977) Biochemistry 16, 3443–3449
12 Kessel, D. (1981) Cancer Res. 41, 1318–1323
13 Berns, M.W., Dahlman, A., Johnson, F.M., Burns, R., Sperling, D., Guiltinan, M., Siemens, A., Walter, R., Wright, W., Hammer-Wilson, M. and Wile, A. (1982) Cancer Res. 42, 2325–2329
14 Salet, C. and Moreno, G. (1981) Int. J. Radiat. Biol. 39, 227–230
15 Santus, R., Kohen, C., Kohen, E., Reyftman, J.P., Morlière, P., Dubertret, L. and Tocci, P.M. (1983) Photochem. Photobiol. 38, 71–77
16 Kessel, D. (1982) Cancer Res. 42, 1703–1706
17 Sandberg, S., Romslo, R., Hovding, G. and Bjorndal, T. (1982) Acta Dermatovener (Stockh.) S100, 75–80
18 Grossweiner, L.I., Patel, A.S. and Grossweiner, J.B. (1982) Photochem. Photobiol. 36, 159–167
19 Grossweiner, L.I. and Goyal, G.C. (1983) Photochem. Photobiol. 37, 529–532
20 Goyal, G.C., Blum, A. and Grossweiner, L.I. (1983) Cancer Res. 43, 5826–5830
21 Grossweiner, L.I. and Goyal, G.C. (1984) J. Photochem. 25, 253–265
22 Margalit, R. and Cohen, S. (1983) Biochim. Biophys. Acta 736, 163–170
23 Jori, G., Tomio, L., Reddi, E., Rossi, E., Corti, L., Zorat, P.L. and Calzavara, F. (1983) Br. J. Cancer 48, 307–309
24 Cozzani, I., Jori, G., Bertoloni, G., Milanesi, C., Carlini, P., Sicuro, T. and Ruschi, A. (1985) Chem. Biol. Interactions 53, 131–143
25 Vever-Bizet, C., Delgado, O. and Brault, D. (1984) J. Chromatogr. 283, 157–163
26 Margalit, R., Shaklai, N. and Cohen, S. (1983) Biochem. J. 209, 547–552
27 Margalit, R. and Rotenberg, M. (1984) Biochem. J. 219, 445–450
28 Falk, J.E. (1964) Porphyrins and Metalloporphyrins, pp. 26–29, Elsevier, Amsterdam
29 Brault, D. and Neta, P. (1983) J. Phys. Chem. 87, 3320–3327
30 Parker, C.A. (1968) Photoluminescence et Solutions, pp. 7–35, Elsevier, Amsterdam
31 Andreoni, A., Cubeddu, R., De Silvestri, S., Jori, G., Laporta, P. and Reddi, R. (1983) Z. Naturforsch. 38c, 83–89
32 Cowled, P.A., Forbes, I.J., Swineer, A.G., Trennery, V.C. and Ward, A.D. (1985) Photochem. Photobiol. 41, 445–451
33 Rougée, M. and Brault, D. (1975) Biochemistry 14, 4100–4106
34 Brault, D., Vever-Bizet, C. and Dellinger, M. (1986) Biochimie, in the press
35 Pottier, R., Laplante, J.P., Chow, Y.F.A. and Kennedy, J. (1985) Can. J. Chem. 63, 1463–1467
36 Bonnett, R., Ridge, R.J. and Scourides, P.A. (1981) J. Chem. Soc., Perkin I, 3135–3140
37 Moan, J. and Sommer, S. (1983) Cancer Lett. 21, 167–174